

Discovery of an ultra-quantum spin liquid

Yanxing Yang

Fudan University

Cheng Tan

Fudan University

Zihao Zhu

Fudan University

J. Zhang

Fudan University

Zhaofeng Ding

Fudan University

Qiong Wu

Fudan University

Changsheng Chen

Fudan University

Toni Shiroka

Paul Scherrer Institut

Douglas MacLaughline

University of California, Riverside

Chandra Varma

University of California-Berkeley

Lei Shu (✉ leishu@fudan.edu.cn)

Fudan University

Article

Keywords: Quantum Fluctuations, Thermodynamic Properties, Muon Relaxation Rates, Invariant Time-dependent Fluctuations, Topological Singlet Excitations

Posted Date: April 2nd, 2021

DOI: <https://doi.org/10.21203/rs.3.rs-351743/v1>

License:  This work is licensed under a Creative Commons Attribution 4.0 International License.

[Read Full License](#)

Discovery of an ultra-quantum spin liquid

Y. X. Yang¹, C. Tan¹, Z. H. Zhu¹, J. Zhang¹, Z. F. Ding¹, Q. Wu¹, C. S. Chen¹, T. Shiroka², D. E. MacLaughlin³, C. M. Varma^{4*}, & L. Shu^{1,5,6*}

¹*State Key Laboratory of Surface Physics, Department of Physics, Fudan University, Shanghai 200433, China*

²*Laboratory for Muon-Spin Spectroscopy, Paul Scherrer Institut, 5232 Villigen, Switzerland*

³*Department of Physics and Astronomy, University of California, Riverside, CA 92521, USA*

⁴*Department of Physics, University of California, Berkeley, CA 94704, USA*

⁵*Collaborative Innovation Center of Advanced Microstructures, Nanjing 210093, China*

⁶*Shanghai Research Center for Quantum Sciences, Shanghai 201315, China*

**Corresponding authors. Email: chandra.varma@ucr.edu (C.M.V.); leishu@fudan.edu.cn (L.S.).*

Quantum fluctuations are expected to lead to highly entangled spin-liquid states in some two-dimensional spin-1/2 compounds. We have synthesized and measured thermodynamic properties and muon relaxation rates in two related such compounds, one of which is the least disordered of this kind synthesized hitherto and reveals intrinsic properties of a class of spin-liquids. Its measured properties can all be simply characterized by scale invariant time-dependent fluctuations with a single parameter. The specific heat divided by temperature and muon relaxation rates are both temperature independent at low temperatures, followed by a logarithmic decrease with increasing temperature. Even more remarkably, $\sim 57\%$ of the magnetic entropy is missing down to temperatures of $O(10^{-3})$ the exchange energy, independent of magnetic field up to $g\mu_B H > k_B T$. This is evidence that quantum fluctuations lead either to a gigantic specific heat peak from topological singlet excitations below such temperatures, or to an extensively degenerate topological singlet ground state. These results reveal an ultra-quantum state of matter.

The study of quantum fluctuations in interacting matter is of primary interest in physics, encompassing fields as diverse as the thermodynamics of black holes^{1,2}, particle physics beyond the standard model³, the theory of quantum computation⁴, and various phenomena in condensed matter physics. The latter is often paradigmatic, since it allows access and control to a wide variety of experiments, and the concepts often cut across different fields. These range from quantum Hall effects⁵ to the quantum criticality that governs high temperature superconductivity^{6,7} to the spin liquid states^{8,9}, all of which have been intensively studied in the last three decades. Spin liquids, in particular, have been hard to characterize beyond the fact that quantum fluctuations prevent

any conventional order in them. Despite extensive experiments, few precise conclusions about the nature of the ground state and low-lying excitations are available, because the results are almost always dominated by cooperative effects, however interesting, of the impurities⁸⁻¹¹.

We have synthesized the $S = 1/2$ triangular lattice compounds $\text{Lu}_3\text{Cu}_2\text{Sb}_3\text{O}_{14}$ (LCSO) and $\text{Lu}_3\text{CuZnSb}_3\text{O}_{14}$ (LCZSO), and measured their thermodynamic properties and muon spin relaxation (μSR) rates $\lambda(T)$ down to 16 mK. In LCSO magnetic impurities are estimated to be less than a part in 10^3 and other impurities or defects about a part in 10^2 . There are no signatures in either compound of conventional or spin-glass order, or any other cooperative effects of impurities down to the lowest temperature. However, a 5% concentration of Schottky defects (Cu/Zn site interchange) in LCZSO is shown to change properties from nearly defect-free LCSO very significantly. We believe the high purity of LCSO allows us to unearth the extraordinary intrinsic properties of a class of spin-liquids.

For $T \ll$ the Weiss temperature $\Theta_W \sim 20$ K, the deduced specific heat $C_M = \gamma T$ from magnetic excitations and $\lambda(T)$ are constants [$\lambda(T \rightarrow 0)$ is related to γ^{-1}], followed by logarithmic decreases with increasing temperature. These results are shown to be consistent with scale-invariant magnetic fluctuations. An even more surprising result is that the *measured* magnetic entropy in LCSO, obtained from the specific heat from 100 mK to its saturation at high temperatures, is only about 36% of the total entropy $k_B \ln 2$ per spin-1/2. μSR measurements effectively extend these results down to 16 mK. The *missing* entropy does not change in a magnetic field up to 9 T at any temperature up to Θ_W . The implications of these results, discussed later, shed a completely new light on the nature of the ground and excited states of a nearly defect-free spin liquid.

We have also synthesized the isostructural nonmagnetic compound $\text{Lu}_3\text{Zn}_2\text{Sb}_3\text{O}_{14}$ (LZSO). LCSO, LCZSO, and LZSO are variations on the $R_3\text{Zn}_2\text{Sb}_3\text{O}_{14}$ series of compounds ($R =$ rare earth)¹², with $R =$ Lu and Zn completely (LCSO) or half (LCZSO) substituted by Cu. So far only powder samples have been synthesized by solid-state reaction methods. All the physical properties shown below have been reconfirmed on independently grown samples.

The crystal structure, lattice dimensions, and x-ray diffraction (XRD) pattern exhibiting narrow Bragg peaks are shown in Supplementary Information (SI) Sec. I for LCSO. The compounds form alternate parallel kagomé planes of Lu and Sb (SI Figs. S1b and S1d). In all three compounds, Cu^{2+} and/or Zn^{2+} ions sit in the slightly distorted hexagons of the Lu^{3+} and Sb^{5+} kagomé layers. The two layers in LCSO have Cu ions in distinct co-ordinations: tetrahedra of Sb (Cu1) and octahedra of Lu (Cu2). In SI Sec. III we show the results of dc and ac susceptibility mea-

surements down to 0.1 K, estimate the magnetic impurity concentrations, and show evidence of no cooperative effects.

LCSO is extraordinarily defect-free, with less than 10^{-3} “orphan” spins and negligible Schottky defects. Static magnetism, ordered or disordered, would be expected from orphan spins, but μ SR experiments rule this out down to ~ 16 mK. LCZSO has alternate planes with primarily Cu in the Lu layers and Zn in the Sb layers. We have not been able to make it with less than 5% substitutional defects, most likely site interchange of Cu and Zn. These are observed in XRD data and give rise to a low-temperature Schottky contribution to the specific heat; they also affect other properties significantly.

In SI Sec. II we discuss the symmetry of the orbitals where the spins reside, which we argue suggests the two-dimensional nature of magnetic interactions in both compounds. Although the details of the microscopic Hamiltonian are not known, the fact that the magnetic susceptibility, the specific heat and the muon relaxation rate in LCSO can all be separated into two distinct components, each characterized by the same two parameters, implies that the exchange interactions in the two layers interact dominantly only with other ions in the same layer. The slight distortions from equilateral of the triangles will lead to slight variations in the exchange interactions in the spatial directions.

Figure 1a shows the measured zero-field specific heat $C(T)$ in LCSO and LCZSO from 60 mK to about 300 K, as well as that of the isostructural nonmagnetic compound LZSO; the latter allows a very accurate subtraction of the lattice contribution C_{latt} . A weak bump in $C(T)$ at about 1 K and an increase below 0.2 K can be seen in both compounds. The low-temperature increase is the expected nuclear Schottky contribution (from quadrupolar splitting in zero applied field) $\propto T^{-2}$, which can be isolated from the bump because the latter is negligible compared to the former at low temperatures. We have carefully investigated the bump. The variation of both the low-temperature increase and the bump with magnetic field are described in SI Sec. IV, where we show that the bump is a Schottky anomaly due to non-magnetic impurities¹³ with an excited magnetic state. All of our conclusions are affected by less than 0.5% whether or not we subtract the Schottky contribution.

The magnetic contribution $C_M(T, H)/T$ is deduced from $C_M/T \equiv [C - (C_{\text{latt}} + C_{\text{nuc}} + C_{\text{imp}})]/T$, where C_{nuc} and C_{imp} are the nuclear and impurity Schottky contributions, respectively. $C_M(T, H)/T$ at various fields is shown in Fig. 1b for LCSO and in SI Fig. S7b for LCZSO. For $H = 0$ $C_M(T)/T$ is constant at low temperatures, below about 0.4 K for LCSO and below about

1 K for LCZSO (SI Fig. S7b). There is an approximately logarithmic decrease with increasing temperature at higher temperatures in both compounds. This and other features are examined in detail in SI Sec. VI, where the logarithmic behavior is shown to be characterized by parameters close to the respective Weiss temperatures.

The results of our specific heat and μ SR measurements are central to the conclusions of this work. In low-temperature specific-heat measurements, especially in insulators, one must ensure that thermal equilibrium is reached in the measurements. The steps we have taken to achieve equilibrium and the evidence for it are described below in the Methods section.

We turn next to the measurable magnetic entropy. Fig. 2a shows the normalized magnetic entropy $[S(T, H) - S(0.1K, H)]/R \ln 2$ calculated by integrating C_M/T from 0.1 K to T . For $H = 0$ it is $\sim 0.36k_B \ln 2$ per spin-1/2 in LCSO at $T = 20$ K. The uncertainty in these numbers is less than 2%. From the proportionality of the μ SR relaxation rate to C_M/T from 16 mK to 4 K (Fig. 3), we infer that the constant C_M/T also continues to at least 16 mK.

The lattice specific heat becomes very large for $T > 20$ K (Fig. 1A), and it is not possible experimentally to obtain the magnetic contribution directly at any higher temperature. In SI Sec. V, we calculate the entropy at $T \approx \Theta_W$ from the high-temperature series expansion for a triangular lattice, and find it be about $0.07k_B \ln 2$ for LCSO. We therefore conclude that either about 57% of the magnetic entropy ($1 - 0.36 - 0.07$) resides in the ground state in LCSO or, more likely, the average C_M/T below ~ 16 mK is about 10^3 times the measured constant value above ~ 100 mK.

At low temperatures the expected decrease $\Delta S_M(T, H) = S_M(T, H) - S_M(T, 0)$ of the entropy with H is observed (Fig. 2a). At temperatures above about 20 K its apparent saturation to a smaller value with field cannot be ascertained accurately by the above subtraction procedure, where as noted above the specific heat is dominated by the lattice contribution. We determine the entropy in a magnetic field by an alternate more accurate method, which also gives an estimate of the accuracy of the subtraction procedure below 20 K.

In the alternate method, the magnetization $M(H, T)$ is measured from 4 K to 300 K at various fields (SI Figs. S4a and S4c). $(\partial M/\partial T)_H$ for both LCSO and LCZSO are given in SI Figs. 4b and 4d. We then use the Maxwell relation $(\partial S/\partial H)_T = (\partial M/\partial T)_H$, and integrate $(\partial S/\partial H)_T$ to give the change in entropy due to the magnetic field as a function of temperature. The results are displayed as red points in Fig. 2b, where the results from the direct determination by subtraction shown in Fig. 2a are shown as black points. To get a measure of the consistency of results obtained by these quite different methods, we note that the standard deviation of the red and black points in

LCSO is 0.02.

The results in Fig. 2b show that the *available* entropy loss due to magnetic fields at low temperatures is systematically recovered asymptotically at higher temperatures to its zero-field value. However, the *missing* entropy is field independent up to 9 T over the whole temperature range. From this behavior at $g\mu_B H \leq k_B T$ it follows that the missing entropy is due to purely singlet excitations. Since it is unaffected even for $g\mu_B H \gg k_B T$ for $k_B T$ larger than the (small) Θ_W , local mutually non-interacting singlet states are also ruled out because their population would be replaced by the doublet states favored by magnetic polarization. We have checked by measuring in a field while both warming and cooling and in cooling in a field and then measuring that the behavior is unchanged; there is no hysteresis. So the phenomena appears not to be due to metastable singlet states.

μ SR is a direct probe of low-energy spin dynamics. We have carried out zero-field (ZF) and longitudinal-field (LF) μ SR measurements from 16 mK to about 20 K in both LCSO and LCZSO, the details of which are discussed in SI Sec. VII. Neither long-range order nor spin freezing were detected down to the lowest temperatures. The ZF dynamic muon spin relaxation rate λ_{ZF} for LCSO is plotted as a function of temperature in Fig. 3. It is essentially constant below about 0.5 K, indicating persistent spin dynamics and a high density of magnetic fluctuations at low temperatures^{14,15}. Also shown is the deduced C_M/T , the temperature dependence of which closely follows that of λ . A temperature-independent relaxation rate as $T \rightarrow 0$ is itself extraordinary. The measured specific heat and its relation to the μ SR relaxation rate suggest a scale-invariant spectral function for magnetic excitations, as discussed below and in SI Sec. X.

We show in the inset in Fig. 3 that the measured $C_M(T)/T$ in LCSO can be separated into two parts for the two layers. The low-temperature constant values for the two layers are approximately inversely proportional to their respective values of Θ_W , and they both decrease logarithmically approximately as $\ln(\Theta_{W1}/T)$ and $\ln(\Theta_{W2}/T)$. The integrated value, i.e. the entropy, is approximately the same for the two layers. These forms only pertain for the ‘quantum region’ below the respective Θ_W ’s. The knee region between the two logarithms requires fit to the semiclassical region $T \gtrsim \Theta_{W2}$. Details are given in SI Sec. VI.

A similar decomposition for LCZSO is given in SI Sec. VIII. Even with only 5% Schottky defects, which are site interchanges of Cu and Zn in the two layers, the ratio of the entropies of the two layers is no smaller than 30%. This emphasizes how important it is to have defect-free compounds to study spin liquids.

Theoretical results for spin liquids and their relation to our experimental findings are summarized in SI Sec. IX. We have not found theoretical results on any relevant model which correspond to the properties discovered here^{8,9}.

Both the specific heat and the μ SR relaxation rate $\lambda(T)$ follow from the scale-invariant density of states function $\mathcal{A}_M(\omega, T) = \gamma_M f(\omega/T)$ for magnetic fluctuations proposed in SI Sec. X. Not only is the temperature dependence of $\lambda(T)$ given by this form, but its order of magnitude is obtained from the same coefficient γ_M that reproduces the magnitude of the measured C_M/T . As a function of imaginary time periodic in inverse temperature, $\mathcal{A}_M(\omega, T)$ is equivalent to an algebraic decay $\propto 1/\tau$. A ground-state entropy, which should more accurately be called a temperature-independent entropy, requires a more singular form $\mathcal{A}_0(\omega, T)$, which corresponds to a correlation function of the singlets approximately proportional to $1/\log(\tau)$. This is as quantum as one can get. Some conceptual questions related to this are briefly discussed in SI Sec. X. This form is chosen in the belief that the missing entropy is due to a dynamical effect. The form can be modified easily by introducing a new scale if instead there are equally unexpected colossal ultra-low energy excitations.

In summary, two related phenomena have been discovered in the nearly defect-free compound LCSO.

(1) Quantitatively related constant C_M/T and μ SR relaxation rates $\lambda(T)$ are observed below a temperature related to the Weiss temperature Θ_W , followed by the same logarithmic cutoff in both measurements. The excitations necessary for these are shown to be scale invariant. They carry finite spin quantum numbers because their entropy for $g\mu_B H \lesssim k_B T$ is systematically reduced due to H ; this leads to constant muon relaxation. They exhaust the *measurable* excitations at all temperatures up to 9 tesla. All measured properties can be related to just the one parameter in the scaling function.

(2) Conclusive evidence is found for *missing* entropy from a colossal density of **singlet** excitations below an ultra-low energy scale compared to the Weiss temperature. Very interesting is also the fact that the ultra-low energy excitations are not removed by a magnetic field as high as 9 Tesla, showing that they are not trivial local singlets but quite probably non-local and topological.

In a close look at the literature (a summary is given in SI Sec. XI), we find that such properties have not been previously observed in any spin-liquid candidates. We think this is because LCSO can be prepared with fewer defects than any other spin liquid investigated so far, so that the intrinsic behavior of a class of spin liquids is revealed. The simplicity and the nature of the

singularities in Eqs. (S9)–(S11), with which we can parameterise all the data, invite important new theoretical developments. The magnetic fluctuations suggested by $\mathcal{A}_M(\omega, T)$ should be accessible via neutron scattering. The detection of the scalar excitations $\mathcal{A}_0(\omega, T)$ poses an interesting challenge to experimental techniques. Having no charge or magnetic moment, they are a form of dark matter not observable by the usual spectroscopic techniques.

References

1. Carlip, S. Black hole thermodynamics. *Int. J. Mod. Phys. D* **23**, 1430023 (2014).
2. Maldacena, J. Black hole entropy and quantum mechanics. *arXiv e-prints* [arXiv:1810.11492] (2018).
3. Ellis, J. Physics beyond the standard model. *Nucl. Phys. A* **827**, 187c – 198c (2009). PANIC08.
4. Li, Y. The theory of quantum computation (2016). (unpublished).
5. Prange, R. & Girvin, S. E. *The Quantum Hall effect* (Springer Verlag, Third Edition, 1990).
6. Varma, C. M. Quantum-critical fluctuations in 2D metals: strange metals and superconductivity in antiferromagnets and in cuprates. *Rep. Prog. Phys.* **79**, 082501 (2016).
7. Varma, C. M. Colloquium: Linear in temperature resistivity and associated mysteries including high temperature superconductivity. *Rev. Mod. Phys.* **92**, 031001 (2020).
8. Broholm, C. *et al.* Quantum spin liquids. *Science* **367**, 263 (2020).
9. Savary, L. & Balents, L. Quantum spin liquids: a review. *Rep. Prog. Phys.* **80**, 016502 (2016).
10. Han, T.-H. *et al.* Thermodynamic Properties of the Quantum Spin Liquid Candidate $\text{ZnCu}_3(\text{OH})_6\text{Cl}_2$ in High Magnetic Fields. *arXiv e-prints* [arXiv:1402.2693] (2014).
11. Kitagawa, K. *et al.* A spin-orbital-entangled quantum liquid on a honeycomb lattice. *Nature* **554**, 341–345 (2018).
12. Sanders, M. B., Krizan, J. W. & Cava, R. J. $\text{RE}_3\text{Sb}_3\text{Zn}_2\text{O}_{14}$ (RE = La, Pr, Nd, Sm, Eu, Gd): a new family of pyrochlore derivatives with rare earth ions on a 2D Kagome lattice. *J. Mater. Chem. C* **4**, 541–550 (2016).
13. He, C. *et al.* Low temperature Schottky anomalies in the specific heat of LaCoO_3 : Defect-stabilized finite spin states. *Appl. Phys. Lett.* **94**, 102514 (2009).

14. Uemura, Y. J. *et al.* Spin Fluctuations in Frustrated Kagomé Lattice System $\text{SrCr}_8\text{Ga}_4\text{O}_{19}$ Studied by Muon Spin Relaxation. *Phys. Rev. Lett.* **73**, 3306–3309 (1994).
15. Ding, Z.-F. *et al.* Possible gapless spin liquid in the rare-earth kagome lattice magnet $\text{Tm}_3\text{Sb}_3\text{Zn}_2\text{O}_{14}$. *Phys. Rev. B* **98**, 174404 (2018).
16. Toby, B. H. & Dreele, R. B. V. *GSAS-II*: the genesis of a modern open-source all purpose crystallography software package. *J. Appl. Crystallogr.* **46**, 544–549 (2013).
17. Li, K. *et al.* Syntheses and properties of a family of new compounds $\text{RE}_3\text{Sb}_3\text{Zn}_2\text{O}_{14}$ (RE=La, Pr, Nd, Sm–Ho) with an ordered pyrochlore structure. *J. Solid State Chem.* **217**, 80 – 86 (2014).
18. Yaouanc, A. & Dalmas de Réotier, P. *Muon Spin Rotation, Relaxation, and Resonance: Applications to Condensed Matter*. International Series of Monographs on Physics (Oxford University Press, New York, 2011).
19. Suter, A. & Wojek, B. M. *musrfit*: A free platform-independent framework for μSR data analysis. *Phys. Procedia* **30**, 69–73 (2012).

Methods

Sample growth and characterization. We have synthesized the compound $\text{Lu}_3\text{Cu}_2\text{Sb}_3\text{O}_{14}$ (LCSO) by the solid state reaction method. Stoichiometric amounts of Lu_2O_3 , CuO and Sb_2O_3 were thoroughly mixed using an agate mortar, and heated to 1030°C for 60 hours with intermediate regrinding and reheating. So far only powder samples could be synthesized. The crystal structure was determined from powder X-ray diffraction (XRD) data taken at room temperature using a Bruker D8 advance XRD spectrometer ($\lambda = 1.5418 \text{ \AA}$). Rietveld refinement of the X-ray data was made using the GSAS program¹⁶.

LCSO belongs to the rhombohedral pyrochlore family^{12,17}, in which kagomé lattices are formed by alternating layers of filled-shell ($S = 0$) Sb^{5+} and Lu^{3+} ions. The spin-1/2 Cu^{2+} ions sit at the centers of the kagomé hexagons (Cu1-Sb and Cu2-Lu). To determine whether the observed properties are specific to the 2D layers, we have also synthesized the related compound $\text{Lu}_3\text{CuZnSb}_3\text{O}_{14}$ (LCZSO), in which nonmagnetic layers, where $S = 0$ Zn ions replace Cu1 and alternate with Cu2 layers. We have been unable to synthesize this compound with less than $\sim 5\%$ site-interchange disorder, despite efforts with different growth protocols.

Magnetic susceptibility measurements. DC magnetic susceptibility measurements above 2 K were made using a Magnetic Property Measurement System (MPMS, Quantum Design). The AC magnetic susceptibility was measured over the temperature range 0.1 K–4 K in a Physical Property Measurement System (PPMS, Quantum Design) equipped with AC susceptibility and dilution refrigerator options. The AC susceptibility measurements covered the frequency range from 631 Hz to 10000 Hz.

Specific heat measurements. Specific heats were measured by the adiabatic relaxation method, using a PPMS equipped with a dilution refrigerator. Data were taken at temperatures between 50 mK and 300 K for LCSO and LCZSO, and 0.2 K–300 K for the isostructural nonmagnetic compound $\text{Lu}_3\text{Zn}_2\text{Sb}_3\text{O}_{14}$ (LZSO). We took special care to ensure that thermal equilibrium was achieved for the low-temperature measurements. As an example, at base temperature (~ 50 mK), the measurement took 70 minutes. The specified PPMS thermal coupling factor between the sample and sample platform was 95% at 100 mK and 99% for temperatures above 0.6 K. Measurements were made during cooling down to base temperature as well as warming up. Similarly, when measuring the specific heat in a magnetic field, the sample was field-cooled and then measured on warming, and also zero-field cooled, field applied at low temperatures, and then measured during warming. The results were always consistent.

Muon spin relaxation experiments. The time-differential μ SR technique¹⁸ was used, in which the evolution of the ensemble muon-spin polarization after implantation into the sample is monitored via measurements of the decay positron count-rate asymmetry $A(t)$. μ SR experiments were performed down to 16 mK using the DR spectrometer on the M15 beam line at TRIUMF, Vancouver, Canada, and the Dolly spectrometer at the Paul Scherrer Institute, Villigen, Switzerland. Samples were attached to a silver cold-finger sample holder in the DR spectrometer, to ensure good thermal contact with the mixing chamber. Appropriate functional forms of $A(t)$ were fit to the asymmetry data using the MUSRFIT μ SR analysis program¹⁹.

Data availability

All data needed to evaluate the conclusions in the paper are present in the main text or the supplementary information.

Acknowledgments

We are grateful to B. Hitti and D. J. Arseneau of TRIUMF and the staff of the Paul Scherrer Institute for their valuable help during the μ SR experiments. C.M.V. performed this work while a “Recalled Professor” at UC Berkeley, and wishes to thank the members of the condensed-matter theory group for their hospitality. This research was funded by the National Research and Development Program of China, No. 2016YFA0300503 and No. 2017YFA0303104, the National Natural Science Foundations of China, No. 11774061, and the Shanghai Municipal Science and Technology (Major Project Grant No. 2019SHZDZX01 and No. 20ZR1405300).

Author contributions

Y.X.Y., C.M.V., and L.S. designed the experiments. Y.X.Y. and J.Z. grew the samples. Y.X.Y. carried out X-ray structure refinement and magnetic characterizations. Y.X.Y., Z.H.Z., and Q.W. performed the specific heat measurements. Y.X.Y., C.T., D.E.M., and L.S. carried out the μ SR experiments, with site assistance from T.S. Y.X.Y., L.S. and C.M.V. analyzed the data. C.M.V. provided the theoretical framework. All authors participated in discussion. The manuscript was written by Y.X.Y., L.S., C.M.V., and D.E.M.

Competing interests

The authors declare no competing interests.

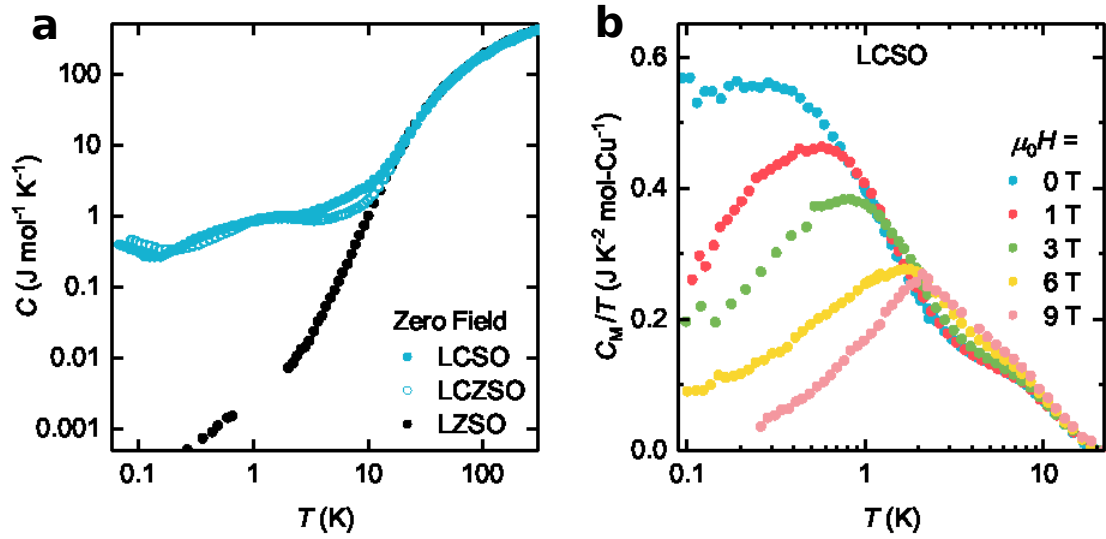


Fig. 1. Specific heat of LCSO, LCZSO, and LZSO. **a**, Measured specific heats in zero field. **b**, Intrinsic magnetic contribution $C_M(T, H)/T$ to the specific heat divided by temperature at various magnetic fields for LCSO, after subtraction of the lattice, nuclear-Schottky, and impurity-Schottky contributions (See text and SI Sec. IV).

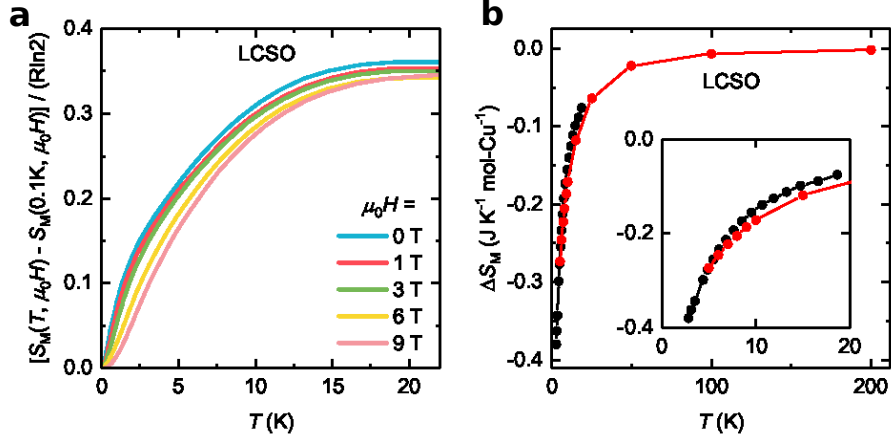


Fig. 2. Entropy of LCSO. **a**, Change $S_M(T, H) - S_M(0.1 \text{ K}, H)$ in magnetic entropy, normalized to $R \ln 2$ per spin, $0.1 \text{ K} \leq T \leq 23 \text{ K}$, $0 \leq H \leq 9 \text{ T}$. **b**, Red symbols: change $\Delta S_M(T, H) = S_M(T, H) - S_M(T, 0)$ in magnetic entropy in an applied field of 9 Tesla as a function of temperature from 2 K to 300 K from measurements of magnetization in LCSO (see text and SI Sec. IV). Black symbols: the same quantity up to 20 K from the direct determination of magnetic entropy shown in Panel **a**. The lost magnetic entropy is fully recovered at high temperatures, proving that the missing entropy is independent of the applied field.

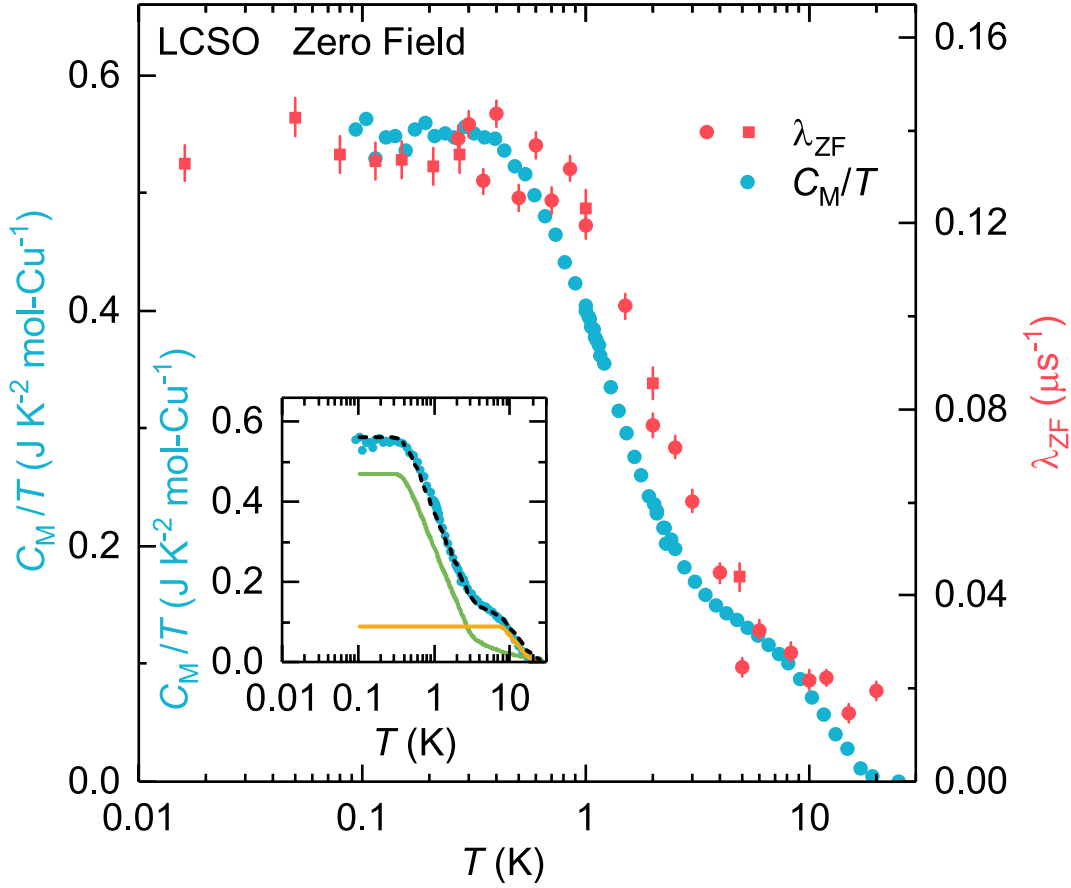


Fig. 3. Muon spin relaxation rate and specific heat in LCSO. A. Temperature dependencies of zero-field muon spin relaxation rate $\lambda(T)$ (red dots: data taken at PSI; red squares: data taken at TRIUMF) and $C_M(T)/T$ (blue dots) at zero field. It is remarkable that the relaxation rate tends to a constant value at low temperatures, and that it follows the temperature dependence of C_M/T over the entire temperature range. Inset: separation of C_M/T into contributions from the two layers (SI Sec. VI). The low-temperature constant values are approximately inversely as their respective Θ_W 's as determined by the fit to the magnetic susceptibility measurements (SI Sec. VI). The characteristic temperatures of the two logarithmic terms are also similar to the respective Θ_W values. The knee between the two logarithms, for $T \gtrsim \Theta_{W2}$ requires a semiclassical form, which we fit to the expression mandated for $T \gg \Theta_W$. With this fit, the *measured* magnetic entropy is consistent with being the same for both layers.

Figures

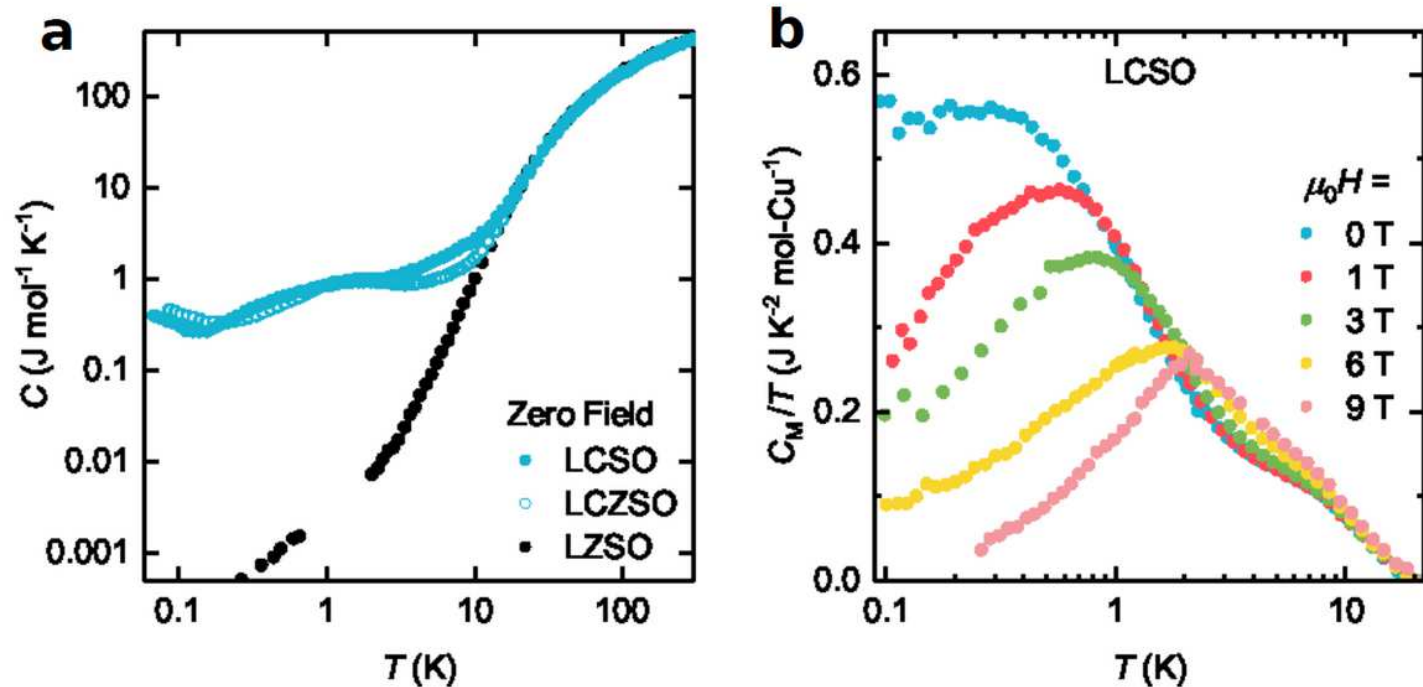


Figure 1

Specific heat of LCSO, LCZSO, and LZSO. a, Measured specific heats in zero field. b, Intrinsic magnetic contribution $C_M(T, H)/T$ to the specific heat divided by temperature at various magnetic fields for LCSO, after subtraction of the lattice, nuclear-Schottky, and impurity-Schottky contributions (See text and SI Sec. IV).

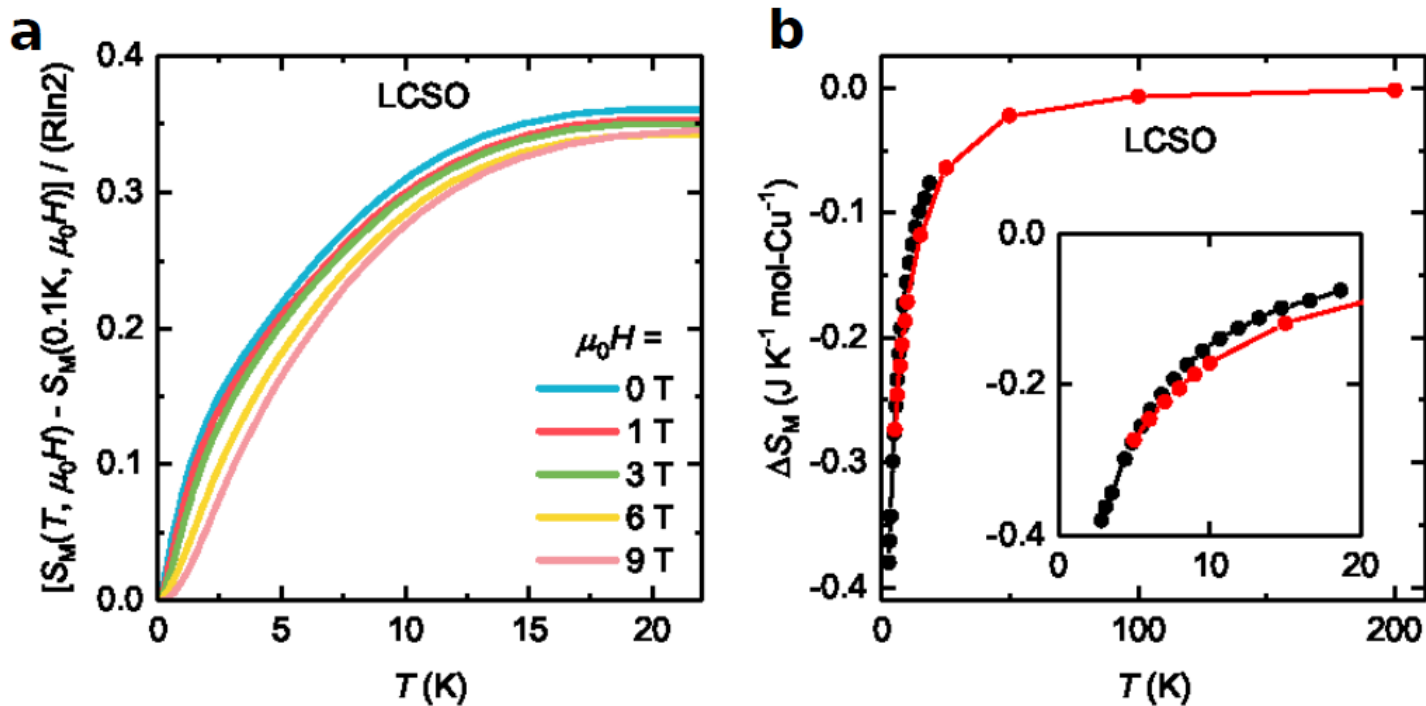


Figure 2

Entropy of LCSO. a, Change $SM(T, H) - SM(0.1 \text{ K}, H)$ in magnetic entropy, normalized to $R \ln 2$ per spin, $0.1 \text{ K} \leq T \leq 23 \text{ K}$, $0 \leq H \leq 9 \text{ T}$. b, Red symbols: change $\Delta SM(T, H) = SM(T, H) - SM(T, 0)$ in magnetic entropy in an applied field of 9 Tesla as a function of temperature from 2 K to 300 K from measurements of magnetization in LCSO (see text and SI Sec. IV). Black symbols: the same quantity up to 20 K from the direct determination of magnetic entropy shown in Panel a. The lost magnetic entropy is fully recovered at high temperatures, proving that the missing entropy is independent of the applied field.

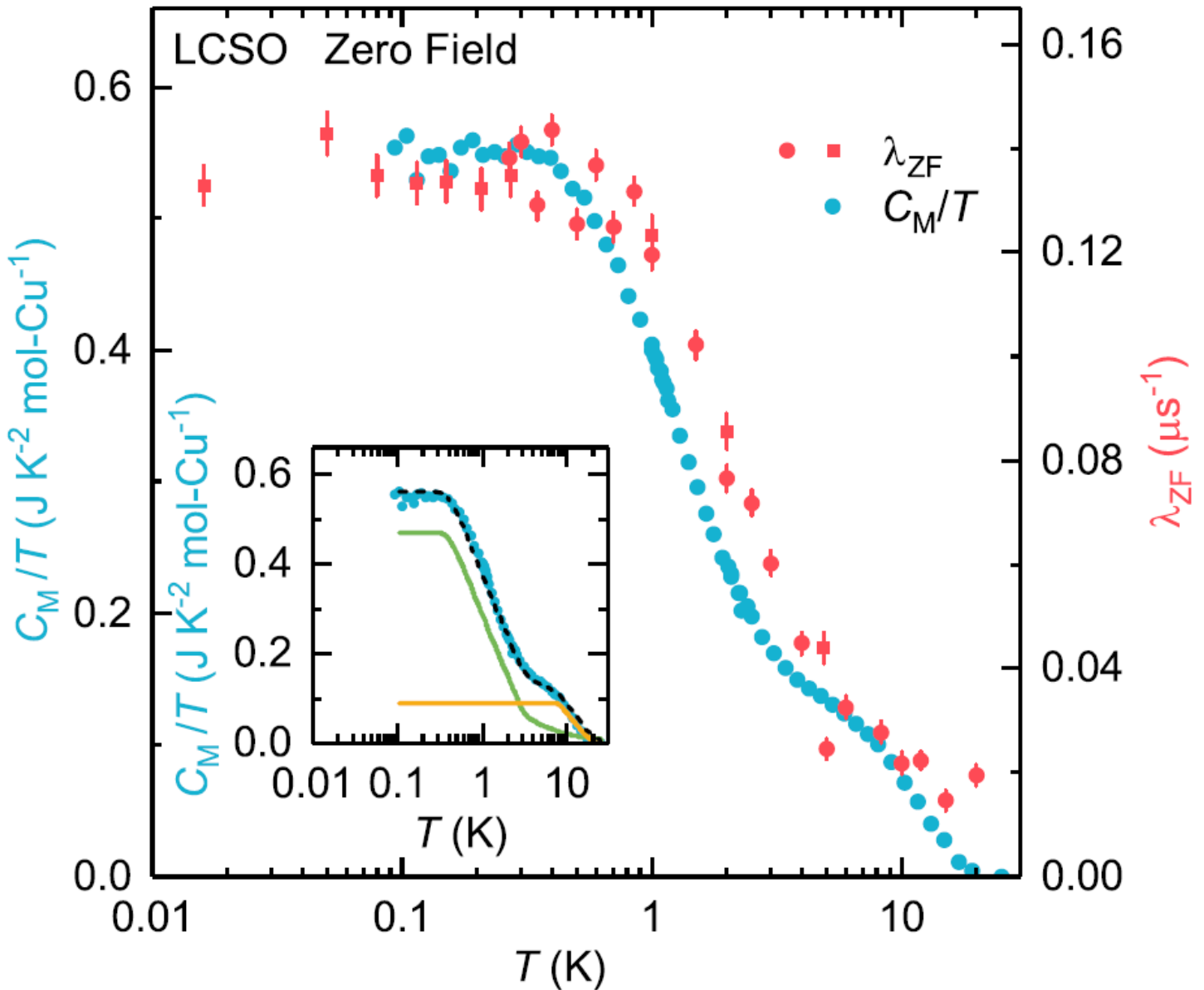


Figure 3

Muon spin relaxation rate and specific heat in LCSO. A. Temperature dependencies of zero-field muon spin relaxation rate $\lambda(T)$ (red dots: data taken at PSI; red squares: data taken at TRIUMF) and $C_M(T)/T$ (blue dots) at zero field. It is remarkable that the relaxation rate tends to a constant value at low

temperatures, and that it follows the temperature dependence of CM/T over the entire temperature range. Inset: separation of CM/T into contributions from the two layers (SI Sec. VI). The low-temperature constant values are approximately inversely as their respective ΘW 's as determined by the fit to the magnetic susceptibility measurements (SI Sec. VI). The characteristic temperatures of the two logarithmic terms are also similar to the respective ΘW values. The knee between the two logarithms, for $T \approx \Theta W^2$ requires a semiclassical form, which we fit to the expression mandated for $T \gg \Theta W$. With this fit, the measured magnetic entropy is consistent with being the same for both layers.

Supplementary Files

This is a list of supplementary files associated with this preprint. Click to download.

- [Suppv11.pdf](#)